RSC Advances

View Article Online
View Journal | View Issue

Effect of conjugation length on fluorescence characteristics of carbon dots†

Jianen Zhang,[a] Mingjun Chen,[a] Xiaojie Ren,[a] Weicai Shi,[a] Tao Yin,[a] Tao Luo,[a] Youshi Lan,[b] Xu Li [ID] *[a] and Li Guan [ID] *[a]

The influence of sp^2- and sp^3-hybridized carbon coexisting in carbon cores on fluorescence characteristics of carbon dots (CDs) was revealed by density functional theory calculations. Based on the constructed coronene-like structures, the fluorescence emission spectra, transition molecular orbital pairs and several physical quantities describing the distribution of electrons and holes were investigated. The results indicate that due to the interaction between sp^2 and sp^3 carbon atoms, two main factors including the hyperconjugative effect and the separation of sp^2 domain by sp^3 carbon atoms can regulate the fluorescence wavelength. By analyzing the transition molecular orbital pairs, it was found that the fluorescence wavelength has a close correlation with the conjugation length, suggesting that the conjugation length can predict the shift of the emission spectra of CDs. The theoretical results provide a comprehensive understanding of fluorescence mechanism and help to synthesize CDs with expected fluorescence wavelength.

1. Introduction

After fullerene nanoballs, carbon nanotubes and graphene, carbon dots (CDs) have become a new hot topic in the research of carbon-based nanomaterials.[1–3] CDs have many peculiar characteristics, including low cost, high stability, easy surface modification, low toxicity, good biocompatibility and tunable photoluminescence, leading to a wide range of applications of CDs.[4–11] In recent years, the relationship between the structure and fluorescence properties of CDs has been widely explored to meet the requirements of practical applications. Many research works have attempted to make the atomic structure of CDs clear and found that CDs mainly consist of carbon cores and surface chemical functional groups.[12–16] Carbon cores are formed by embedding sp^2-hybridized graphene fragments in a sp^3-hybridized carbon network.[17,18] Therefore, there are two main methods to regulate the fluorescence emission wavelength of CDs. One is to change the size of the carbon cores, the other is to modify surface functional groups of CDs.[19–21] The main purpose of changing the size of the carbon cores is to change the range of the sp^2 carbon domains, which can determine the energy gap of CDs.[22,23] Hence, many previous investigations focused on the structures of carbon cores and their influence on fluorescence properties. Experimentally, polycyclic aromatic hydrocarbons (PAHs) are mostly used to construct the carbon cores composed by sp^2-hybridized carbon atoms.[24–27] Recently, some researchers realized the fluorescence shift of CDs by changing hybridization types of carbon.[28–31] Lu et al.[32] regulated the external pressure to achieve an irreversible change from yellow (557 nm) to blue-green (491 nm) emission of CDs. To explain this phenomenon, N-doping polyaromatic structures were produced to model the N-doping CD structure, and first-principles calculations performed at the B3LYP/6-31G(d) level proved that the fluorescence blueshift originated from the transformation of sp^2 into sp^3-hybridized domains under high pressure. Rukhlenko et al.[33] simulated the CD structure by pairs of coupled polycyclic aromatic molecules and concluded that with the increase of the sp^2-hybridized carbon domains in sp^3-hybridized amorphous core, the valence electrons become more delocalized and thus the fluorescence redshift occurs by using a simple quantum chemical approach. Wang et al.[19] changed the number of sp^2 hybridized benzene rings in the sp^3 carbon network to modulate the sp^2/sp^3 ratio and demonstrated that the conversion of sp^3-hybridized to sp^2-hybridized leads to the emission redshift of CDs using first-principles calculations at the B3LYP/6-31G(d) level. Recently, Xu et al.[34] used acetic acid to promote the formation of sp^3 carbons during the synthesis of CDs. They designed a variety of sp^2 hybridized benzene ring structures to evaluate the effect of conjugated rings on the emission wavelength and found as the number of conjugated rings increases from 1 to 25, the calculated energy gap energy decreases resulting from electron delocalization within the sp^2

[a]Key Laboratory of High-precision Computation and Application of Quantum Field Theory of Hebei Province, College of Physics Science and Technology, Hebei University, Baoding 071002, PR China. E-mail: lguan@hbu.edu.cn; lixcn@sina.com
[b]Department of Radiochemistry, China Institute of Atomic Energy, Beijing 102413, PR China

domain using first-principles calculations performed at the B3LYP/6-31G(d) level.

The above-mentioned theoretical and experimental works have found that the proportion of sp^2- and sp^3-hybridized carbon has a regulating effect on the fluorescence properties of CDs. However, the influence of sp^2-conjugated domains surrounded by sp^3 carbon core on fluorescence emission still needs further discussion. In this work, coronene-like structures consisting of sp^2-hybridized benzene rings and sp^3-hybridized carbons were constructed. The electronic structures and fluorescence emission spectra were calculated by using density functional theory (DFT) and time-dependent density functional theory (TD-DFT) methods. Firstly, the relationship between the geometry configuration of carbon cores and fluorescence spectra was investigated and the interaction between sp^2- and sp^3-hybridized carbon atoms was discussed in details. Then, the correlation of the conjugation length and the fluorescence emission was revealed by analyzing the transition molecular orbitals. This work illustrates the effect of sp^2 and sp^3 hybridized carbon on the fluorescence emission of CDs and provides a theoretical guidance for the controlled synthesis of CDs.

2. Models and computational details

All calculation works were performed by Gaussian 16 package[35] and performed by using the range-separated hybrid function ωB97X-D[36] with dispersion correction in conjunction with the def2-SVP[37] basis set. The polarizable continuum model (PCM) solvation approach was used to calculate the solvation effect in aqueous solution using the self-consistent reaction field method.[38] More computational details and the choice of calculation method with basis set are in the ESI.† As shown in Fig. 1, coronene structure was selected to construct various sp^2- and sp^3-hybridized carbon cores. Here, the size of sp^2 carbon domain was controlled by changing the number of sp^2-hybridized benzene rings. Single-electron excitation was considered to describe the radiative transitions, and three structures in spin-triplet state were excluded shown in Fig. S1† in the ESI.† The ground-state geometry and electronic structure optimizations were carried out by DFT calculations with no constraints imposed beyond the multiplicity of the electronic state. Frequency calculations were performed to check the local energy minimum. Then the excited-state geometries were further optimized by linear-response TD-DFT method.[39] The vertical excitation energy and oscillator intensity of the electronic transitions in fluorescence spectra were also obtained. To verify the validity of theoretical method, the fluorescence emission energy of coronene was firstly calculated, and the theoretical value 3.35 eV is in agreement with the experimental value 2.95 eV.[40] The electronic properties analysis of all models were finished by Multiwfn 3.8 software.[41]

3. Results and discussion

3.1 Emission properties of CDs

Fig. 2 shows the calculated fluorescence emission spectra of all models. Previously experimental and theoretical works have
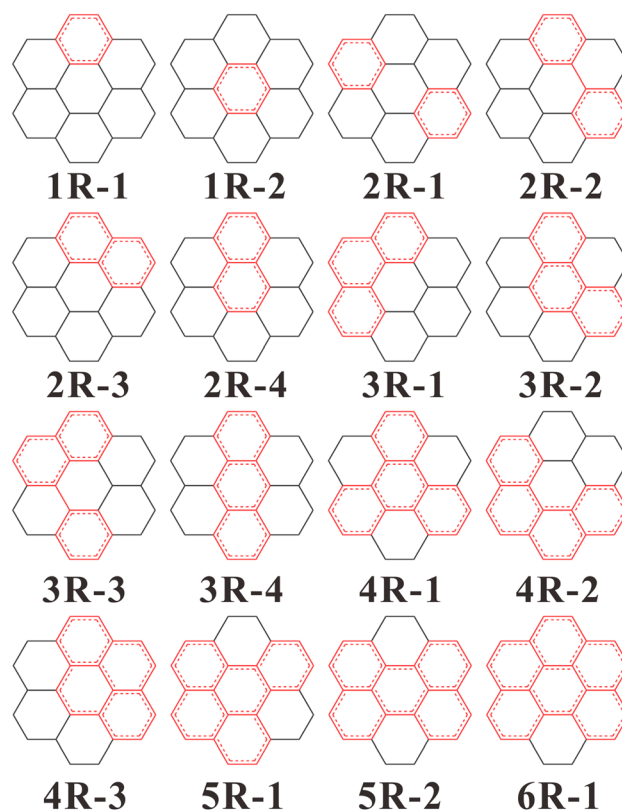

Fig. 1 Structures of coronene-like carbon dot models. Red rings represent sp^2-hybridized benzene rings. nR (n = 1, 2, …, 6) represents the number of sp^2 carbon rings, and nR-i represents the i-th structure with n sp^2 rings.

revealed that the fluorescence wavelength of CDs shows a redshift trend with the increasing content of sp^2 carbon domain.[19,42] In this work, the content of sp^2-hybridized carbon domain can be evaluated as the number of sp^2 carbon rings. From structures 1R-i to 6R-i, the content of sp^2 carbon domain varies from 25% to 92%. In overall view, the fluorescence
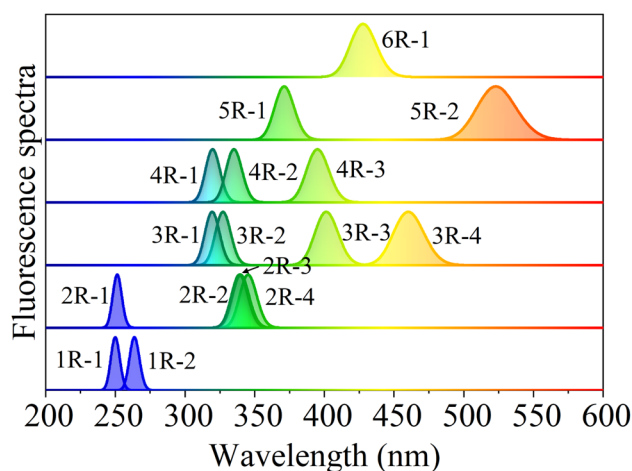

Fig. 2 Calculated normalized fluorescence spectra of coronene-like structures.

wavelengths (250–523 nm) of all models exhibit a rough redshift trend with the increasing content of sp^2-hybridized carbon. However, it should be noted that the emission wavelength and the content of sp^2 domain are not strictly related. Sometimes, the more content of sp^2 domain corresponds to the shorter emission wavelength, or the same content of sp^2 domain produces different emission wavelength. The results suggest that the size of sp^2 domain is not the only reason for regulating the fluorescence shift.

Analyzing the geometry configuration illustrated as Fig. 1, it can be found that structures 1R-1 and 1R-2 with the same content of sp^2 domain have different but close fluorescence emission peaks located at 250 nm and 264 nm, respectively. Also, structures 2R-3 and 2R-4, structures 3R-1 and 3R-2 with the same content of sp^2 carbon have different but close emission peaks. Observing these structures, one can see that they have the same content and geometry configurations of sp^2 domain but different sp^3-hybridized carbon surrounding networks. The results mean that although the content of sp^2 carbon domain is unchanged, various sp^3 surrounding structures can induce the fluorescence emission shift of carbon cores.

In Fig. 2, another interesting result is that different contents of sp^2 carbon domains possibly causes similar fluorescence wavelengths. For example, structure 2R-1 exhibits an emission peak at 251 nm, which is very close to the peak position of structure 1R-1 or 1R-2. Comparing their benzene ring configurations, one can see that although structure 2R-1 has two sp^2-hybridized rings, the two rings are separated by sp^3-hybridized carbon atoms, suggesting that the two benzene rings are essentially independent. Therefore, the completely-separated sp^2 carbon domains in carbon core behave as smaller individual domains, which finally determines the fluorescence wavelength. This phenomenon has been observed in experimental measurement, where the fluorescence emission was dictated by isolated small sp^2 domains.[43] Nonetheless, it should be noted that the sp^2 carbon domains in some cases seem to be separated, but the benzene rings are factually linked by C–C single bonds. For example, the sp^2 carbon domains in structures 2R-2 and 3R-3 are not completely separated, which leads to the fluorescence emission energies of the two structures different from any smaller individual domains such as structure 1R-1 or 2R-4. Thus, the conclusion is not suitable for describing the separated sp^2 domains linked by C–C single bonds.

As we all know, zigzag edges and arm-chair edges are two typical edges of sp^2 carbon domain in CDs. In the present models, structures 2R-4, 3R-4 and 5R-2 have zigzag edges and exhibit long-wavelength fluorescence emission compared to other structures with the same content of sp^2 domain. By contrast, structures 3R-1, 4R-1 and 5R-1 have arm-chair edges and exhibit short-wavelength fluorescence emission among all structures with the same content of sp^2 domain. The results indicate that when the content of sp^2 domains remains unchanged, the structures with zigzag edges exhibit long-wavelength emission compared with the ones with arm-chair edges, which is consistent with the theoretical results.[42] For those structures with both edge features, the fluorescence emission peaks are located between the two situations mentioned above. From the perspective of aromatic stabilization, the zigzag and arm-chair structures exhibit obvious differences, and the former is more susceptible to chemical reaction and has lower aromatic stabilization than the latter.[44] The calculated spectra in Fig. 2 indicate that when the content of sp^2 domain is the same, the higher the stability of CDs, the shorter the fluorescence wavelength.

3.2 Electron excitation characters of CDs

In order to give a deeper understand of the excitation properties of CDs, the transition energy, oscillator strength, fluorescence wavelength and the configuration interaction contributions of molecular orbitals mainly involved in electronic transitions are summarized shown as Table 1. The highest occupied molecular orbital (HOMO)–the lowest unoccupied molecular orbital (LUMO) transition contributions of 9 models (2R-2, 2R-3, 2R-4, 3R-3, 3R-4, 4R-3, 5R-1, 5R-2 and 6R-1) approach 100%, which indicates that the fluorescence emissions of these structures are mainly dominated by the HOMO to LUMO transitions. The electron transitions of the remaining 7 structures are contributed by 2–3 groups of orbitals pairs near HOMO and LUMO.

The hole–electron distribution is introduced by analyzing the weights of electronic transitions of molecular orbitals.[45,46] According to Kasha's rule, the first excited state of singlet state is usually the critical state for emitting fluorescence.[47] Therefore, the hole–electron distribution is applied to evaluate the electronic emission process from the first excited state to the ground state. Table 2 shows that the values of the relevant physical quantities describing the distribution of electrons and holes for CDs, and the explanations and formulas for these physical quantities are shown in the ESI.† It can be found that the average value of charge transfer distance (D) for all structures is 0.11 Å and the maximum value is 0.433 Å. Due to the C–C bond length is about 1.4 Å, so the small charge transfer distance indicates that the centers of mass of electrons and holes are very close. S_r index measures the degree of electron–hole overlap, and the calculated minimum value 0.82 means that the distributions of holes and electrons mostly overlap. Therefore, according to the values of D and S_r, it can be judged that the fluorescence emissions of all structures belong to local excitation.[48,49] Moreover, all the overall spatial distribution scope $\Delta\sigma$ are close to 0 and the electron–hole separation degree t are negative, which implies that there is no significant separation of the hole and electron. In a word, the above analysis gives a clear explanation that the excitation of all models belongs to a local excitation dominated by π–π^* transitions, which suggests that one effective approach for regulating fluorescence spectrum of CDs is to change the π-conjugated sp^2 carbon domains.

3.3 The relationship between conjugation length and fluorescence emission

In order to further describe the fluorescence properties of carbon core structures, all the orbital pairs mainly involved in

Table 1 Transition energy, oscillator strength, fluorescence wavelength, and configuration interaction (CI) contributions (major molecular orbitals involvement, %) of all models. Here, HOMO and LUMO are denoted as H and L, respectively

Structure	Transition energy (eV)	Oscillator strength (f)	λ_{em} (nm)	Configuration interaction contribution (%)					
1R-1	4.96	0.022	250	H → L	62.7%	H−1 → L+1	30.7%		
1R-2	4.70	0.008	264	H−1 → L	54.7%	H → L+1	39.1%		
2R-1	4.93	0.021	251	H → L+1	51.3%	H−2 → L	19.9%	H−1 → L+1	11.9%
2R-2	3.66	0.664	339	H → L	97.8%				
2R-3	3.59	0.289	340	H → L	98.9%				
2R-4	3.65	0.360	345	H → L	98.9%				
3R-1	3.88	0.018	319	H → L+1	61.6%	H−1 → L	33.4%		
3R-2	3.79	0.058	327	H → L+1	48.8%	H → L	21.3%	H−1 → L	19.4%
3R-3	3.09	0.556	401	H → L	98.2%				
3R-4	2.69	0.333	460	H → L	99.5%				
4R-1	3.87	0	320	H → L	49.4%	H-1 → L+1	46.1%		
4R-2	3.70	0.005	335	H → L+1	55.6%	H-1 → L	36.9%		
4R-3	3.14	0.970	395	H → L	98.1%				
5R-1	3.34	0.817	371	H → L	96.0%				
5R-2	2.37	0.636	523	H → L	98.7%				
6R-1	2.90	0.617	428	H → L	97.8%				

Table 2 Charge transfer distance (D, Å), overlap degree (S_r), overall spatial distribution difference ($\Delta\sigma$) and separation degree (t, Å) of all structures

Structure	D	S_r	$\Delta\sigma$	t
1R-1	0.058	0.91	0.044	−1.261
1R-2	0.124	0.89	0.181	−1.395
2R-1	0.038	0.89	0.032	−1.767
2R-2	0.197	0.88	−0.006	−1.511
2R-3	0.006	0.92	0.112	−0.978
2R-4	0.074	0.82	0.114	−1.107
3R-1	0.433	0.86	0.027	−1.322
3R-2	0	0.89	−0.037	−1.585
3R-3	0.012	0.89	0.031	−1.548
3R-4	0.155	0.85	0.043	−1.556
4R-1	0.267	0.88	0.020	−1.865
4R-2	0.009	0.91	0.011	−2.094
4R-3	0.362	0.87	−0.026	−1.535
5R-1	0.024	0.88	0.055	−2.132
5R-2	0	0.87	0.089	−2.491
6R-1	0.098	0.86	0.063	−2.006

electronic transitions were calculated. Fig. 3 shows main transition molecular orbital pairs for the fluorescence emission process of the coronene-like structures. According to the distribution of molecular orbitals, one can see that the sp² carbon domain is the main source of fluorescence emission, and the sp³ carbon atoms adjacent to sp² domain also contribute to the electronic transition process, whereas the sp³ carbon atoms away from the sp² domains have a lesser immediate impact on the fluorescence.

The sp² carbon domains are constructed from PAHs, and hence the fluorescence emission of carbon core is closely related to C=C double bonds. The conjugation length is defined as the number of C=C bonds on the shortest path between two terminal carbon atoms.[50] For conjugated molecules, sp² carbon domain belongs to a π-conjugated system,

and its conjugation length is helpful to understand the optical properties.[51] The relationship between conjugation length and fluorescence emission is significant for understanding the fluorescence characteristics and synthetizing CDs with tunable luminescence. For simple PAHs, the conjugation length can be directly given by evaluating C=C double bonds *via* valence bond theory. However, CDs have complex structures containing PAHs and sp³ carbon atoms, and a reasonable conjugation length needs to be estimated by molecular orbitals calculations.

Fig. 3 shows that in HOMO, C=C double bonds are in bonding states and C–C single bonds are in anti-bonding states, whereas in LUMO, the bonding and anti-bonding states are reverse. If a six-membered ring demonstrates the molecular orbital characteristics of benzene, its conjugation length is 2. Based on the calculated occupied orbitals of models given in Fig. 3, the values of conjugation lengths are determined by evaluating the number of C=C double bonds on the shortest path between two terminal carbon atoms and the configuration interaction contribution is considered in the present calculations.

In order to make clear the influences of sp³ carbon atoms on fluorescence wavelength, the fluorescence spectra of corresponding PAHs without sp³-hybridized carbon atoms were calculated and the geometric structures of corresponding PAHs are shown in Fig. S2 in the ESI.† According to the transition molecular orbital pairs of all coronene-like and PAHs structures, the conjugation lengths were evaluated and Fig. 4 gives the relationship between the conjugation length N and fluorescence wavelength. In Fig. 4, one can see that the conjugation length of any coronene-like structure is equal to that of corresponding PAHs, suggesting that when the sp² carbon domain is fixed, the sp³ carbon network has no substantial influence on the conjugation length. For two groups of structures, the change trend of the emission wavelength is consistent with that of the conjugation length, suggesting that fluorescence emission is
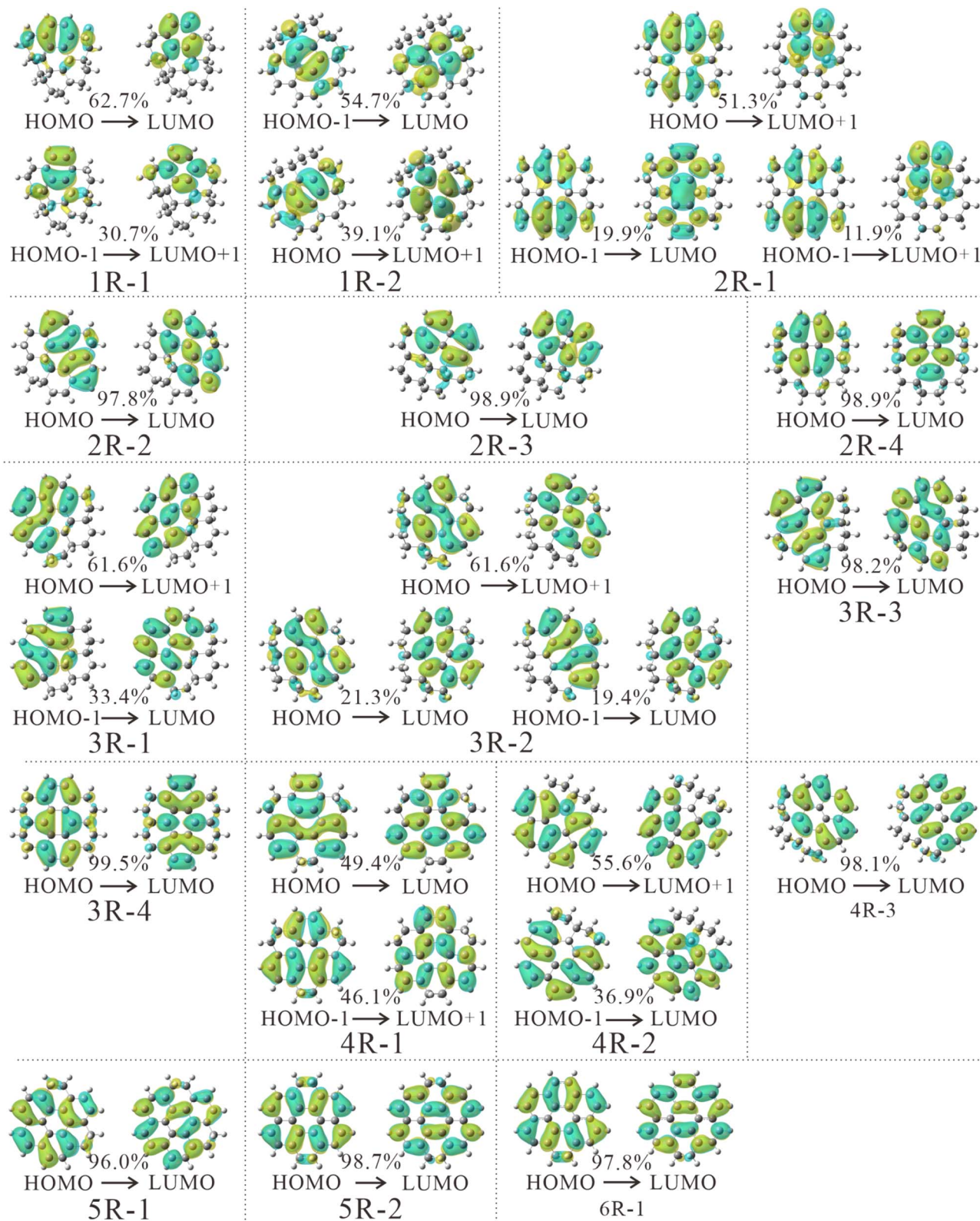
Fig. 3 Main transition molecular orbital pairs from the fluorescence emission process of all coronene-like structures. The positive and negative phases of molecular orbitals are portrayed by the colours cyan and yellow, respectively.

highly correlated with the conjugation length N. The longer conjugation length, the longer fluorescence wavelength, and *vice versa*. The results demonstrate that besides PAHs containing sp^2-hybridized carbon, the conjugation length also is suitable to characterize the fluorescence wavelength of carbon core structures with sp^2- and sp^3-hybridized carbon.
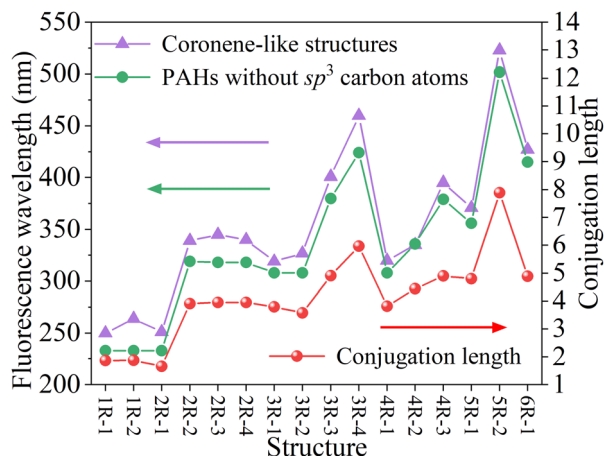
Fig. 4 The relationship between conjugation length and fluorescence wavelength of the coronene-like structures and the corresponding PAHs without sp³ carbon atoms.

Fig. 5 Fluorescent emission energy *versus* 1/*N* of coronene-like structures and corresponding PAHs. Curves: Kuhn fit. Dash lines: linear fit.

Additionally, shown as in Fig. 4, the emission wavelengths of all coronene-like structures are always longer than those of corresponding PAHs. The differences between two groups of fluorescence wavelengths are in the range of 11–36 nm. The result indicates that when the sp² carbon domain keeps unchanged, the surrounding sp³ carbon atoms can cause a little fluorescence redshift of carbon cores. Combined with the analysis of molecular orbital pairs in Fig. 3, it is found that the influence of sp³ carbon atoms mainly originates from the hyperconjugative effect. This conclusion also can explain the small wavelength difference between the structures with the same content of sp² carbon such as 1R-1 and 1R-2 shown as Fig. 2.

The conjugation length of π-conjugated system does not increase infinitely. When the conjugation length is short, the fluorescence wavelength and the conjugation length show a linear relationship.[50] With the increase of sp² carbon domain and conjugation length, the fluorescence wavelength gradually reaches a limit value, that is, the fluorescence emission no longer undergoes red shift.[52,53] The longest conjugation length was defined as effective conjugation length.[50,54] Based on the relationship between the fluorescence emission energy and the reciprocal of conjugation length 1/*N*, Kuhn fit and linear fit can be applied to obtain the effective conjugation length of conjugated polymers.[50] Details about the Kuhn fit are in the ESI.† In order to further characterize the effective conjugation length of CDs, Fig. 5 gives that fluorescent emission energy *versus* 1/*N* of coronene-like structures and the corresponding PAHs. According to the analysis of electron–hole distribution in Table 2, and it is concluded that the electronic transition of coronene-like structures belongs to local excitation, suggesting that Kuhn fit is suitable to describe these systems. One can see that when the value of 1/*N* is greater than about 0.1, the fluorescence emission energies of all the structures display a linear relationship with 1/*N*, which further explains the linear relationship between the size of sp² carbon domain and fluorescence wavelength observed in previous research works about CDs.[42]
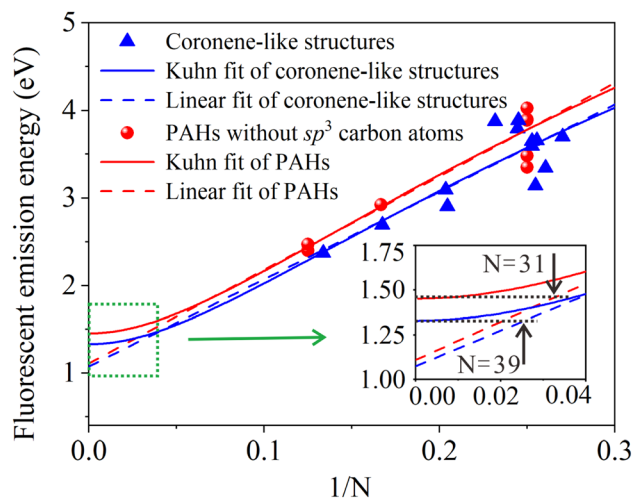
Additionally, the present simulation in Fig. 5 shows that when 1/*N* gradually approaches 0, the fluorescence emission energy reaches a minimum value. The result tells us that with the increase of sp² carbon domain, the fluorescence wavelength will reach a limit. For the coronene-like structures, the minimum fluorescence emission energy 1.33 eV can be obtained by Kuhn fit and linear fit, the effective conjugation length is 39, and the corresponding size of carbon core is 10.4 nm. For PAHs structures, the fitting minimum fluorescence emission energy is 1.45 eV, correspondingly, the effective conjugation length is 31 and the effective size of PAHs is 8.3 nm. The results are in good agreement with the fitting minimum emission energy 1.53 eV, the effective conjugation length 36, and the effective size 9.6 nm obtained from experimental data of PAHs,[44] as shown in Fig. S3 in the ESI.† The results suggest that effective conjugation length can be helpful to predict the minimum fluorescence emission energy and effective size of carbon cores. Moreover, compared with PAHs and coronene-like structures, it is found that when sp² carbon domains are surrounded by sp³ carbon, the fluorescence redshift can be induced, hence the emission energy of coronene-like structures is always less than that of PAHs structure. In a word, the conjugated length has a dominant effect on the fluorescence wavelength shift of carbon core, which helps to further analyze the relationship between the sp² carbon domain and fluorescence spectrum.

4. Conclusions

In order to further understand the fluorescence characteristics of CDs, the coronene-like structures with various sp²-hybridized benzene rings and sp³ carbon network were constructed, and the electronic properties and fluorescence spectra were calculated by DFT and TD-DFT methods. The results revealed that when the content of sp² domains in carbon cores is the same, the influence of sp³ carbon atoms is mainly reflected in the

hyperconjugative effect and the separation of sp^2 domain by sp^3 carbon atoms, which causes a small fluorescence shift of carbon cores. The sp^2 domains with zigzag edges have longer fluorescence wavelength compared with the ones with arm-chair edge due to lower aromatic stabilization.

Analyzing the correlation between the conjugation length and fluorescence emission, it was found that the longer the conjugation length, the longer the fluorescence wavelength. Related to the size of sp^2 carbon domains, the conjugation length is more convenient to predict the fluorescence emission shift trend of CDs. Moreover, based on the relationship between the fluorescence emission energy and $1/N$, Kuhn fit and linear fit can be applied to predict the effective conjugation length and effective fluorescence size of CDs. This work provides a deeper understand about the influence of sp^3 carbon atoms and the conjugation length of sp^2 domain on the fluorescence properties of CDs.

Author contributions

The manuscript was written through contributions of all authors. All authors have given approval to the final version of the manuscript.

Conflicts of interest

The authors declare no competing financial interest.

Acknowledgements

References

1 S. Li, L. Li, H. Tu, H. Zhang, D. S. Silvester, C. E. Banks, G. Zou, H. Hou and X. Ji, *Mater. Today*, 2021, **51**, 188–207.

2 J. Liu, R. Li and B. Yang, *ACS Cent. Sci.*, 2020, **6**, 2179–2195.

3 N. Baig, I. Kammakakam and W. Falath, *Mater. Adv.*, 2021, **2**, 1821–1871.

4 J. Yu, X. Yong, Z. Tang, B. Yang and S. Lu, *J. Phys. Chem. Lett.*, 2021, **12**, 7671–7687.

5 I. S. Raja, S. J. Song, M. S. Kang, Y. B. Lee, B. Kim, S. W. Hong, S. J. Jeong, J. C. Lee and D. W. Han, *Nanomaterials*, 2019, **9**, 1214.

6 J. Du, N. Xu, J. Fan, W. Sun and X. Peng, *Small*, 2019, **15**, e1805087.

7 S. Y. Lim, W. Shen and Z. Gao, *Chem. Soc. Rev.*, 2015, **44**, 362–381.

8 G. Li, C. C. Lin, W.-T. Chen, M. S. Molokeev, V. V. Atuchin, C.-Y. Chiang, W. Zhou, C.-W. Wang, W.-H. Li, H.-S. Sheu, T.-S. Chan, C. Ma and R.-S. Liu, *Chem. Mater.*, 2014, **26**, 2991–3001.

9 J. Liao, M. Wang, F. Lin, Z. Han, B. Fu, D. Tu, X. Chen, B. Qiu and H. R. Wen, *Nat. Commun.*, 2022, **13**, 2090.

10 L. Wu, X. Tian, K. Deng, G. Liu and M. Yin, *Opt. Mater.*, 2015, **45**, 28–31.

11 H. Zheng, Z. Zhao, J. B. Phan, H. Ning, Q. Huang, R. Wang, J. Zhang and W. Chen, *ACS Appl. Mater. Interfaces*, 2020, **12**, 2145–2151.

12 H. J. Yoo, B. E. Kwak and D. H. Kim, *Carbon*, 2021, **183**, 560–570.

13 F. Yuan, Z. Wang, X. Li, Y. Li, Z. Tan, L. Fan and S. Yang, *Adv. Mater.*, 2017, **29**, 1604436.

14 X. Miao, D. Qu, D. Yang, B. Nie, Y. Zhao, H. Fan and Z. Sun, *Adv. Mater.*, 2018, **30**, 1704740.

15 H. Li, S. Han, B. Lyu, T. Hong, S. Zhi, L. Xu, F. Xue, L. Sai, J. Yang, X. Wang and B. He, *Chin. Chem. Lett.*, 2021, **32**, 2887–2892.

16 J. Deb, D. Paul and U. Sarkar, *J. Phys. Chem. A*, 2020, **124**, 1312–1320.

17 J. E. Abraham and M. Balachandran, *J. Fluoresc.*, 2022, **32**, 887–906.

18 E. A. Stepanidenko, I. A. Arefina, P. D. Khavlyuk, A. Dubavik, K. V. Bogdanov, D. P. Bondarenko, S. A. Cherevkov, E. V. Kundelev, A. V. Fedorov, A. V. Baranov, V. G. Maslov, E. V. Ushakova and A. L. Rogach, *Nanoscale*, 2020, **12**, 602–609.

19 B. Wang, J. Yu, L. Sui, S. Zhu, Z. Tang, B. Yang and S. Lu, *Adv. Sci.*, 2020, **8**, 2001453.

20 P. Li, S. Xue, L. Sun, X. Zong, L. An, D. Qu, X. Wang and Z. Sun, *Light: Sci. Appl.*, 2022, **11**, 298.

21 H. Ding, X.-X. Zhou, J.-S. Wei, X.-B. Li, B.-T. Qin, X.-B. Chen and H.-M. Xiong, *Carbon*, 2020, **167**, 322–344.

22 L. Jiang, H. Ding, M. Xu, X. Hu, S. Li, M. Zhang, Q. Zhang, Q. Wang, S. Lu, Y. Tian and H. Bi, *Small*, 2020, **16**, 2000680.

23 Z. Sun, F. Yan, J. Xu, H. Zhang and L. Chen, *Nano Res.*, 2021, **15**, 414–422.

24 E. V. Kundelev, N. V. Tepliakov, M. Y. Leonov, V. G. Maslov, A. V. Baranov, A. V. Fedorov, I. D. Rukhlenko and A. L. Rogach, *J. Phys. Chem. Lett.*, 2020, **11**, 8121–8127.

25 L. F. Melia, S. D. Barrionuevo and F. J. Ibañez, *J. Chem. Educ.*, 2022, **99**, 745–751.

26 M. Fu, F. Ehrat, Y. Wang, K. Z. Milowska, C. Reckmeier, A. L. Rogach, J. K. Stolarczyk, A. S. Urban and J. Feldmann, *Nano Lett.*, 2015, **15**, 6030–6035.

27 E. V. Kundelev, N. V. Tepliakov, M. Y. Leonov, V. G. Maslov, A. V. Baranov, A. V. Fedorov, I. D. Rukhlenko and A. L. Rogach, *J. Phys. Chem. Lett.*, 2019, **10**, 5111–5116.

28 X. Duan, Z. Ao, H. Zhang, M. Saunders, H. Sun, Z. Shao and S. Wang, *Appl. Catal., B*, 2018, **222**, 176–181.

29 C. Hu, T. J. Lin, Y. C. Huang, Y. Y. Chen, K. H. Wang and K. Y. Andrew Lin, *Environ. Res.*, 2021, **197**, 111008.

30 M. Cao, X. Zhao and X. Gong, *Small*, 2022, **18**, e2106683.

31 W. Ren, J. Bai, T. Cai, S. Li, E. Pang, H. Zhang and Z. Li, *Opt. Mater.*, 2021, **115**, 111064.

32 S. Lu, G. Xiao, L. Sui, T. Feng, X. Yong, S. Zhu, B. Li, Z. Liu, B. Zou, M. Jin, J. S. Tse, H. Yan and B. Yang, *Angew Chem. Int. Ed. Engl.*, 2017, **56**, 6187–6191.

33 N. V. Tepliakov, E. V. Kundelev, P. D. Khavlyuk, Y. Xiong, M. Y. Leonov, W. Zhu, A. V. Baranov, A. V. Fedorov, A. L. Rogach and I. D. Rukhlenko, *ACS Nano*, 2019, **13**, 10737–10744.

34 J. Xu, Q. Liang, Z. Li, V. Y. Osipov, Y. Lin, B. Ge, Q. Xu, J. Zhu and H. Bi, *Adv. Mater.*, 2022, **34**, e2200011.

35 M. Frisch, G. Trucks, H. Schlegel, G. Scuseria, M. Robb, J. Cheeseman, G. Scalmani, V. Barone, G. Petersson and H. Nakatsuji, *Gaussian 16, revision C.01*, Gaussian Inc., Wallingford, CT, 2016.

36 J. D. Chai and M. Head-Gordon, *Phys. Chem. Chem. Phys.*, 2008, **10**, 6615–6620.

37 F. Weigend and R. Ahlrichs, *Phys. Chem. Chem. Phys.*, 2005, **7**, 3297–3305.

38 S. Miertuš, E. Scrocco and J. Tomasi, *Chem. Phys.*, 1981, **55**, 117–129.

39 C. Adamo and D. Jacquemin, *Chem. Soc. Rev.*, 2013, **42**, 845–856.

40 B. Shi, D. Nachtigallova, A. J. A. Aquino, F. B. C. Machado and H. Lischka, *J. Phys. Chem. Lett.*, 2019, **10**, 5592–5597.

41 T. Lu and F. Chen, *J. Comput. Chem.*, 2012, **33**, 580–592.

42 M. A. Sk, A. Ananthanarayanan, L. Huang, K. H. Lim and P. Chen, *J. Mater. Chem. C*, 2014, **2**, 6954–6960.

43 C. T. Chien, S. S. Li, W. J. Lai, Y. C. Yeh, H. A. Chen, I. S. Chen, L. C. Chen, K. H. Chen, T. Nemoto, S. Isoda, M. Chen, T. Fujita, G. Eda, H. Yamaguchi, M. Chhowalla and C. W. Chen, *Angew Chem. Int. Ed. Engl.*, 2012, **51**, 6662–6666.

44 R. Rieger and K. Müllen, *J. Phys. Org. Chem.*, 2010, **23**, 315–325.

45 Z. Liu, T. Lu and Q. Chen, *Carbon*, 2020, **165**, 461–467.

46 T. Le Bahers, C. Adamo and I. Ciofini, *J. Chem. Theory Comput.*, 2011, **7**, 2498–2506.

47 M. Kasha, *Discuss. Faraday Soc.*, 1950, **9**, 14–19.

48 U. J. Undiandeye, H. Louis, T. E. Gber, T. C. Egemonye, E. C. Agwamba, I. A. Undiandeye, A. S. Adeyinka and B. I. Ita, *J. Indian Chem. Soc.*, 2022, **99**, 100500.

49 Y. Zhang, C. Shen, X. Lu, X. Mu and P. Song, *Spectrochim. Acta, Part A*, 2020, **227**, 117687.

50 J. Gierschner, J. Cornil and H. J. Egelhaaf, *Adv. Mater.*, 2007, **19**, 173–191.

51 B. Milián-Medina and J. Gierschner, *Wiley Interdiscip. Rev.: Comput. Mol. Sci.*, 2012, **2**, 513–524.

52 H. Okamoto, in *Physics and Chemistry of Carbon-Based Materials*, 2019, ch. 7, pp. 211–228, DOI: **10.1007/978-981-13-3417-7_7**.

53 F. B. Mallory, K. E. Butler, A. C. Evans, E. J. Brondyke, C. W. Mallory, C. Yang and A. Ellenstein, *J. Am. Chem. Soc.*, 1997, **119**, 2119–2124.

54 H. Meier, U. Stalmach and H. Kolshorn, *Acta Polym.*, 1997, **48**, 379–384.